One-Pot Synthesis of Benzo[4,5]imidazo[1,2-a]pyrimidin-2-ones Using a Hybrid Catalyst Supported on Magnetic Nanoparticles in Green Solvents

Alkassoume Moussa[a] and Abbas Rahmati*[b]

The conversion of soluble polyoxometalate into insoluble polyoxometalate is considered to be one of the major challenges in synthetic organic chemistry. Here, polyoxometalate was bonded to the salt part of an organic branch immobilized on the silica-coated Fe_3O_4 nanoparticle and characterized using various techniques. The fabricated complex was used as a heterogeneous catalyst in a novel one-pot reaction for synthesis of benzo[4,5]imidazo[1,2-a]pyrimidin-2-ones using aromatic amines, dimethyl acetylenedicarboxylate (DMAD), derivatives of benzaldehyde and 2-aminobenzimidazole in water/ethanol as a green solvent. 21 derivatives of benzo[4,5]imidazo[1,2-a]pyrimidin-2-one were synthesized by this method and fully characterized. The high stability of the catalyst showed that it can be reused for 6 times without decreasing in activity. The combination of new synthetic method, new ferromagnetic heterogeneous nano-catalyst, green solvent and simple separation method were presented in this work.

1. Introduction

A green chemistry approach entails that chemical products and processes are designed in a way that reduce or eliminate the use and/or generation hazardous materials from the environment.[1] In recent years, the green chemistry (Green ChemisTREE) has grown and it was converted to an enormous tree.[2] Green solvents, heterogeneous catalysts, and one-pot syntheses are important branches of green chemistry based approaches.

The utilization of green solvents such as ionic liquids, deep eutectic solvents, liquid polymers, fluorous solvents, water, and nontoxic organic solvents such as ethanol has been well documented in synthesis of organic compounds.[3–6] Water is one of the most important green solvents used for organic syntheses due to its efficiency, eco-friendly nature, non-toxicity, low cost, availability, and easy performance as well as its positive effects on the rate, time and yield of the reaction and selectivity of organic transformations. Also, the reaction proceeds in the presence of the lower amount of catalyst by using this green solvent.[7]

The use of heterogeneous catalysts instead of homogeneous catalysts has increased in both laboratories and industry due to easy separation, decreasing of the corrosion, stability and catalytic activity as well as economic and environmental advantages.[8–11] Keggin-type heteropolyacids (HPAs) are homogeneous catalysts which were widely applied in organic transformations.[12,13] The fixation of these soluble heteropolyacids on insoluble inorganic-organic hybrid magnetic nanoparticles via covalent bonds not only makes heterogeneous catalyst but also creates a large contact surface and improves flexibility of branches of HPA.[14,15]

Recently, attention to one-pot reactions has increased due to complex molecules constructed from readily available starting materials in one-pot without separation of intermediates.[16,17] Multicomponent reactions, a sub group of one-pot reactions, are divided into three categories entitled domino, sequential and consecutive reactions.[18] In consecutive multicomponent reactions, conditions are changeable and intermediates are isolable, but no separation takes place due to the one-pot nature of the reactions.[19] Thus, these processes are very important in the economic, environmental and industrial fields and from the viewpoint of the green chemistry.[20] Various MCRs are applied to synthesize heterocyclic molecules in the presence and absence of catalysts.[21,22]

Benzimidazo[1,2-a]pyrimidines are an important category of N-fused heterocycles containing pyrimidine and benzimidazole rings.[23] Benzimidazopyrimidines have also been reported as pyrimidobenzimidazoles in literature.[23–25] They have widely biological properties such as antibacterial,[26] antiviral,[27] antifungal,[28] antiulcer,[29] anti-HIV,[30] anticancer,[31,32] antiproliferative[33] and anti-inflammatory[34] activities. For treatment of Alzheimer disease, some of these compounds have been applied as allosteric enhancer of acetylcholine affinity at

[a] A. Moussa
Department of Chemistry
University of Isfahan
Isfahan (Iran)

[b] Dr. A. Rahmati
Department of Chemistry
University of Isfahan
P. O. Box 81746-73441
Isfahan, (Iran)
E-mail: a.rahmati@sci.ui.ac.ir

ChemistryOpen

Full Papers
doi.org/10.1002/open.202100063

Chemistry Europe
European Chemical
Societies Publishing

muscarinic M_3 receptor,[35] imaging agent for detecting neurological disorders[36] and protection against amyloid β associated neurotoxicity.[37] They are also used as NK1 receptor antagonist for treatment of schizophrenia disease.[38] These molecules bind to DNA via π-π interactions and prohibits replication of DNA double helix.[39] Moreover, pyrimido[1,2-a]benzimidazole-5(6H)-ones have been used as potent and orally active inhibitors of lymphocyte specific kinase.[40] Hydrated benzimidazo[1,2-a]pyrimidines have been shown antineoplastic activity against some of the human anticancer cell lines.[41] Thus synthesis of these compounds are very important. A three-component reaction has been reported by ourselves in 2005.[42] In this reaction, 4H-pyrimido[2,1-b]benzazoles are synthesized using 2-aminobenzimidazole, an aldehyde, and a β-ketoester in the presence of 1,1,3,3-N,N,N',N'-tetramethylguanidinium trifluoroacetate as an ionic liquid (Scheme 1). This approach has been developed by other groups using various catalysts and conditions.[43–50] In the rest of these works, we report a new consecutive four-component reaction for the synthesis of 3,4-dihydrobenzo[4,5]imidazo[1,2-a]pyrimidin-2(1H)-ones by successive addition of aniline, DMAD, benzaldehyde derivatives and 2-aminobenzimidazole in the presence of new organic-inorganic hybrid nanomagnetic catalyst in water/EtOH as a green solvent.
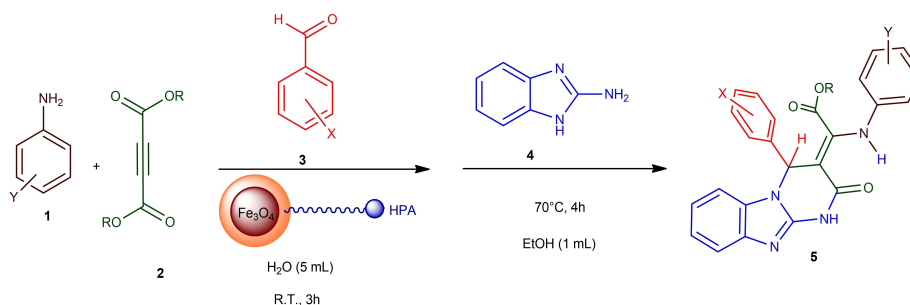
2. Results and Discussion

2.1. Synthesis and Characterization of NM-SiO₂@SiPA-MA-Arg @HPA Catalyst

NM-SiO₂@SiPA-MA-Arg@)HPA, as a nanomagnetic organic-inorganic hybrid catalyst, was prepared as depicted in Scheme 2. Initially, Fe_3O_4 magnetic nanoparticles (MNPs) were fabricated by aqueous co-precipitation manner using $FeCl_2.4H_2O$ and $FeCl_3.6H_2O$ compounds. Then, the surface of nanomagnet was coated by silica, after that triethoxysilylpropyl amine was immobilized onto the surface of afforded coated-MNPs. These inorganic-organic nanomagnetic particles reacted with maleic anhydride and then with arginine and resulted in the formation of a supported compound NM-SiO₂@SiPA-MA-Arg. On the other hand, a solution of heteropoly acid-containing zinc atom was produced using the reported method in literature from Na_2HPO_4, $Na_2WO_4.2H_2O$ and Zn(II) nitrate salt in water in the presen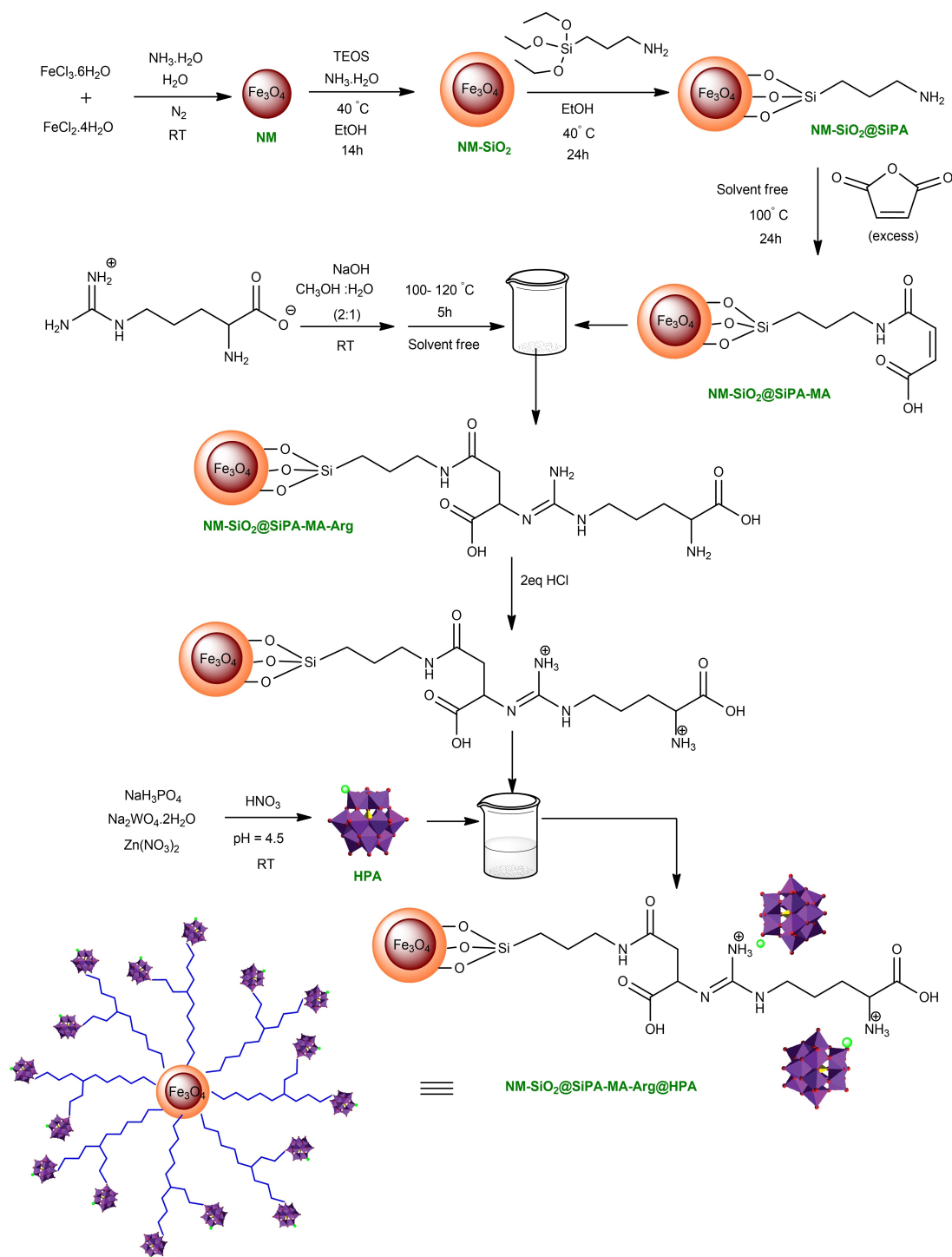ce of HNO_3 at pH of 4.8. Finally, this solution was added to the supported ionic liquid in water very slowly.[51] Immediately, a bulk precipitate was generated and it was washed several times using water and ethanol until the final catalyst was obtained. The formation of the catalysts was proved using various techniques such as EA, FT-IR, SEM, TEM, EDX and VSM.

Initially, elemental analysis techniques such as flame atomic absorption (FAA), inductively coupled plasma-optical emission spectrometry (ICP-OES), and CHNS elemental analysis method were used to prove the structures of the nanomagnetic compounds (intermediates including NM, NM-SiO₂, NM-SiO₂@SiPA, NM-SiO₂@SiPA-MA and NM-SiO₂@SiPA-MA-Arg) and final catalyst (NM-SiO₂@SiPA-MA-Arg@HPA). Table 1, shows the elemental percentage in the structures in every stage by various techniques. Results confirm that all layers were successively immobilized. Also, results show that the amount of iron percentage decreased at every stage by addition of the layers (Entries 1 and 5, Table 1). Also, EA revealed that wt% of the C and N atoms are 2.54 and 1.05% in the structure of the catalysts. Correspondingly, analyses with AA revealed that wt% of the Fe, W, Zn, and P atoms are 14.50, 40.41, 1.42, and 1.20% in the structure of the catalyst, respectively. These results are almost confirmed by ICP-OES technique. Some water molecules exist in the surface or cavities of intermediates in form of chemisorbed and/or physisorbed, to eliminate these physisorbed water molecules and also to decrease the calculation error, the sample is heated at 120–150°C for 5 hours, before using in every stage. Next, they were cooled down to room temperatures while it was fully controlled. These results confirm the successful bonding of these molecules to previous immobilized molecules. Results showed that the amount of phosphorus is higher than the actual amount. Probably, some phosphate ions are adsorbed to silica surface physically.

Synthesis steps of the intermediates and NM-SiO₂@SiPA-MA-Arg@HPA were also confirmed by the FT-IR spectra. The spectrum of Fe_3O_4 (NM) showed two characteristic absorptions at 632 and 558 cm⁻¹ due to the Fe-O-Fe vibrations. After coating with a layer of SiO₂, the FT-IR spectrum of Fe_3O_4@SiO₂ (NM-SiO₂) proved the addition of another peak at 1059. The presence of the broad absorption signals around 3431 or 3392 indicates O−H stretching vibrations representing a strong intermolecular hydrogen bond in both cases. The presence of SiPA was demonstrated by the absorption peak at 2924 cm⁻¹ related to the stretching vibrations of CH_2 bonds. Also, the broad band at 1049 cm⁻¹ is due to Si-O-C and C-N vibrations

Scheme 1. One-pot synthesis of 3,4-dihydrobenzo[4,5]imidazo[1,2-a]pyrimidin-2(1H)-ones.

ChemistryOpen

Full Papers
doi.org/10.1002/open.202100063

Chemistry Europe
European Chemical
Societies Publishing

**Scheme 2.** Synthesis of the NM-SiO$_2$@SiPA-MA-Arg@)HPA catalyst.

which have overlapped. Peaks at 1704, 1604 and another peak at 1439 cm^{-1} correspond to stretching vibrations of C=O, C=C and N—CO groups showed the addition of maleic anhydride on NM-SiO$_2$@SiPA. The FT-IR spectrum of NM-SiO$_2$@SiPA-MA-Arg showed the bands at about 2750–350 and 1650 cm^{-1} assigned to the stretching of the carboxylic acid and guanidine part of arginine. Based on the literature, the observed stretching frequencies at 891, 951 and 1079 cm^{-1} are attributed to P—O,

W=O and W—O—W bands of the terminal oxygen of polyoxometalate moiety, respectively.[52,53] The latter signal has overlapped with strong stretching frequencies of CH$_2$. These bands demonstrate the construction of the final catalyst. (Figure 1)

The immobilization of the organic part and HPA onto the Fe$_3$O$_4$ magnetic nanoparticle was confirmed by EDX spectrum (Figure 2). This spectrum revealed the presence of the O, C, N, Zn, Fe, Si, P and W elements in the structure of the catalyst. EDX
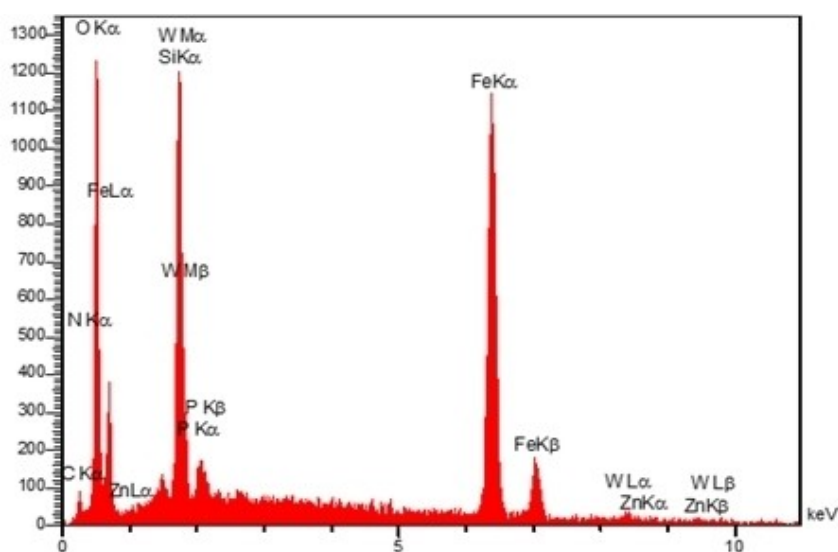
ChemistryOpen

Full Papers
doi.org/10.1002/open.202100063

Chemistry Europe
European Chemical
Societies Publishing

Table 1. Determination of element wt% in intermediates and catalyst by various methods.

Entry	Technique	Portion	NM	NM-SiO2	NM-SiO2@SiPA	NM-SiO2@SiPA-MA	NM-SiO2@SiPA-MA-Arg	NM-SiO2@SiPA-MA-Arg @HPA
1	FAA	Fe %	69.80%	39.92%	36.22%	33.65%	31.40%	14.50%
2		W %	–	–	–	–	–	40.41%
3		Zn %	–	–	–	–	–	1.42%
4		P %	–	–	–	–	–	1.20%
5	ICP-OES	Fe %	71.04%	38.87%	35.36%	32.98%	31.59%	13.91%
6		Si %	–	16.34%	17.19%	16.81%	16.23%	7.21%
7		W %	–	–	–	–	–	41.07%
8		Zn %	–	–	–	–	–	1.29%
9		P %	–	–	–	–	–	1.14%
10	CHNS	C %	–	–	2.17%	4.29%	6.27%	2.54%
11		H %	0.44%	1.19%	1.41%	1.64%	2.05%	0.98%
12		N %	–	–	0.84%	0.84%	2.41%	1.05%
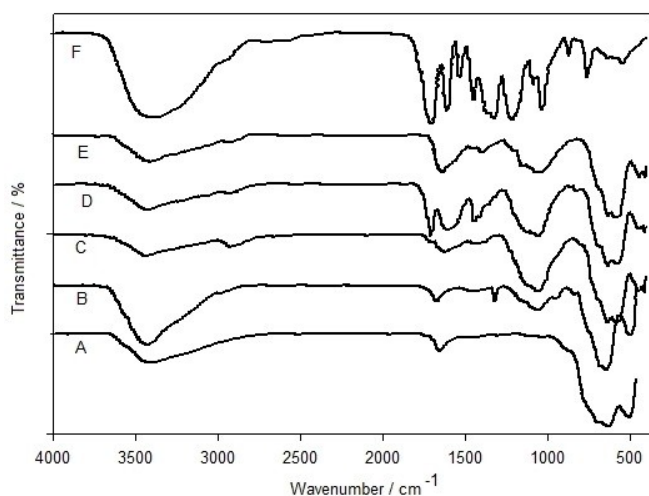
Figure 1. FT-IR: NM (A), NM-SiO$_2$ (B), NM-SiO$_2$@SiPA (C), NM-SiO$_2$@SiPA-MA (D), NM-SiO$_2$@SiPA-MA-Arg (E) and NM-SiO$_2$@SiPA-MA-Arg@)HPA (F).

mapping analysis of NM-SiO$_2$@SiPA-MA-Arg@HPA catalyst showed the spatial distribution of the different atoms taken one by one in the catalyst and the mixture of all atoms in the catalyst (Figure 3). The morphology of the catalyst was further identified by FE-SEM analysis (Figure 4A, B). SEM images showed that particles of the catalyst are relatively uniform and spherical. Also, the size of the particles differs almost from 20–30 nm. Also, TEM images clearly illustrates the structure of the synthesized catalyst were spherical and nanoscale. The average particle size confirmed the results of SEM. The TEM images showed that the core of the nanoparticles is nanomagnet and the shell of the nanoparticle has been covered using organic structures (Figure 4C, D).

The magnetism of the catalyst was tested by VSM analysis (Figure 5). Comparison of the magnetism of the NM, NM-SiO$_2$@SiPA-MA-Arg and NM-SiO$_2$@SiPA-MA-Arg@HPA displayed a difference of 10 emu/g for NM and NM-SiO$_2$@SiPA-MA-Arg and 5 emu/g for NM-SiO$_2$@SiPA-MA-Arg and NM-SiO$_2$@SiPA-MA-Arg @HPA. The results indicated that the magnetizations decreased by addition of the organic layers and HPA on to the Fe$_3$O$_4$ magnetic nanoparticle. This weak magnetization is due

Figure 2. EDX pattern of NM-SiO$_2$@SiPA-MA-Arg@HPA catalyst.

ChemistryOpen

Full Papers
doi.org/10.1002/open.202100063

Chemistry
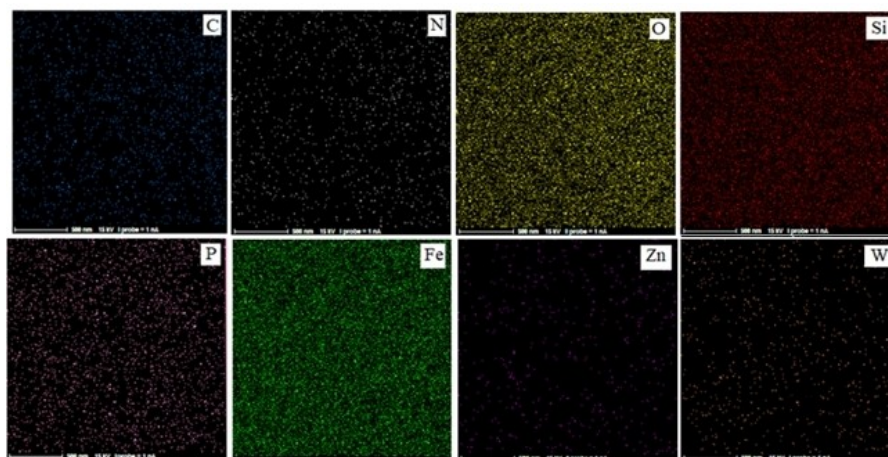**Europe**
European Chemical
Societies Publishing

Figure 3. MAP images of spatial distribution of the carbon, nitrogen, oxygen, silicium, phosphorus, iron, zinc, tungsten atoms in NM-SiO$_2$@SiPA-MA-Arg@HPA.
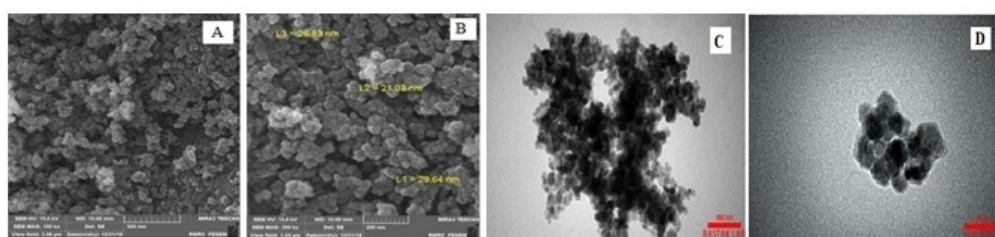

Figure 4. SEM images of NM-SiO$_2$@SiPA-MA-Arg@HPA catalyst as magnetic nanoparticle in two different scale(A, B). TEM image of NM-SiO$_2$@SiPA-MA-Arg@HPA core/shell in two different scale (C, D).
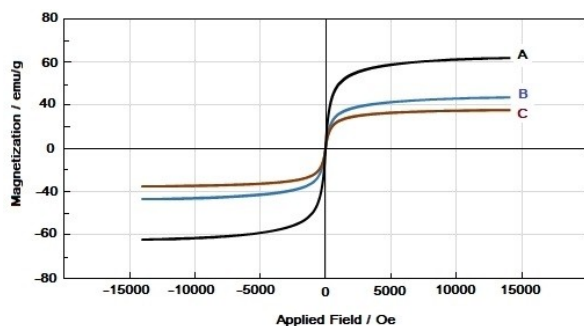

Figure 5. The VSM measurements of Fe$_3$O$_4$ (A), NM-SiO$_2$@SiPA-MA-Arg (B), NM-SiO$_2$@SiPA-MA-Arg@HPA (C).

first to a weak fixation of the organic chain. Also to the length of this chain witch is too long as well as its flexibility decreasing the obstacle to the magnetic fields.

Thermal gravimetric analysis (TGA) of the NM-SiO$_2$@SiPA-MA-Arg@HPA was investigated to study its thermal decomposition (Figure 6A). The sample was heated from 40 °C to 830 °C at 10 °C/min, and showed three main stages. The first small weight loss of 1.81% at 150 °C is assigned to removal of physically adsorbed water and surface hydroxyl groups, and the second weight loss about 4.63% at 330 °C is probably due to

the decomposition of organic groups. The last stage shows a weight loss about 3.56% from 330 to 600 °C resulting from the decomposition of organic spacer grafting to the Fe surface. To determine the amount, type and distribution of acid sites, temperature-programmed desorption of ammonia (NH$_3$-TPD) technique was used. The applied gas in this process was He monitored by the FTIR apparatus. Before each NH$_3$-TPD experiment, the catalyst was degassed using He at 300 °C in a flow of 10 sccm during 1 hour, and cooled down to 110 °C. Next, 65 mg of the catalyst placed in a U-shaped quartz reactor, followed by the adsorption of 5% NH$_3$/He at 110 °C for 30 min. The sample was then purged in a He stream for 30 min at 110 °C in order to remove loosely bond ammonia. Then, the sample was heated again from 110 °C to 800 °C at a heating rate of 10 °C/min in a flow of He (10 sccm). The curve (Figure 6B) shows three areas corresponding to three range of temperature. The first small area (31.92) at 100 to 300 °C range is related to the organic acids (carboxylic acid groups). The second area (421.18) is assigned to acidic sites of heteropolyacid about 300–600 °C. Finally, the adsorbed NH$_3$ at 600 to 800 °C range corresponds to the strong Lewis acids sites in which created by Zn substituted HPA and possibly defects in HPA structures.
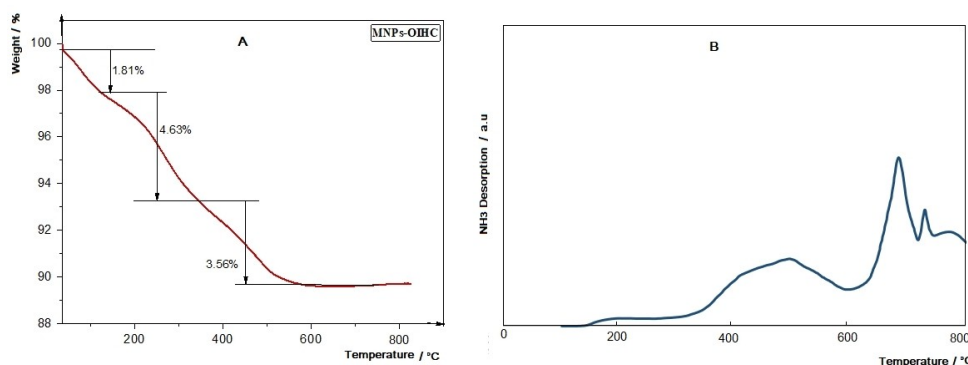
ChemistryOpen

Full Papers
doi.org/10.1002/open.202100063

**Chemistry
Europe**
European Chemical
Societies Publishing

Figure 6. The TGA (A) and TPD (B) curve of NM-SiO$_2$@SiPA-MA-Arg@HPA.

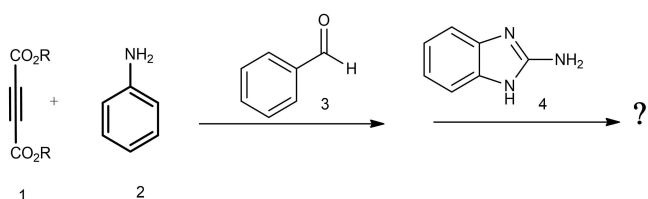## 2.2. Synthesis of Benzoimidazo[1,2-*a*]Pyrimidin-2-one with NM-SiO$_2$@SiPA-MA-Arg @HPA Catalyst

Based on our previous work,[42] a new reaction was designed for synthesis of benzoimidazo[1,2-*a*]pyrimidin-2-one. In this reaction, an enamine-one was synthesized in situ from the reaction of aromatic amine and dialkyl acetylenedicarboxylate and used as a C–H acid instead of β-ketoester (scheme 3).

The designed multicomponent reaction was studied in ethanol under reflux condition. After 24 h, in the absence of the catalyst monitoring of the reaction by the TLC showed that no product was created. Then, the efficiency of the NM-SiO$_2$@SiPA-MA-Arg@HPA catalyst was studied in the proposed reaction. TLC revealed that some products were generated in this stage. Separation of products showed that the yield of one of them was be more than the others (23%). The obtained product was characterized by IR, ^{1}H NMR and ^{13}C NMR spectra as well as elemental analysis. It was found that the product is benzo[4,5] imidazo[1,2-*a*]pyrimidin-2-one. This result encourages us to do more investigation about this synthesis. All efforts including to change solvent and temperature as well as catalyst amount to improve the yield of the reaction failed in the case of domino process. For this reason, the reaction was done in form of a consecutive four-component reaction. Consequently, the reaction of an aniline with DMAD was done without any separation. This step of reaction was performed very fast. It is important to note that the reaction between aniline and DMAD is exothermic, so DMAD should be added drop by drop at room temperature. Next, aldehyde was added and followed by TLC. This step proceeded very hard and was not completed even after 24 h in the absence of the catalyst. The rate of reaction

was increased and completed in the short time (2 h) when the catalyst was used. Next, 2-aminobenzimidazole was added to the reaction medium and followed by TLC. It showed that the reaction was completed at considerable time. It was decided to optimize systematically the reaction conditions such as the solvent and temperature as well as catalyst amount.

At first, the model reaction (aniline, DMAD, benzaldehyde and 2-aminobenzimidazole) was done as consecutive four-component reaction in several solvents in the presence of NM-SiO$_2$@SiPA-MA-Arg@HPA catalyst under reflux conditions (Table 2). The results showed that the protic solvents are almost better than the others. Among them the water was the best solvent. When ethanol as co solvent was added to water the reaction yield was extremely increased. Thus, mixture of water/ethanol was chosen as reaction media. Next, the effect of the temperature was checked on the yield of reaction (Table 2, Entries 8–11). Results showed that the temperature plays an important role in this approach. When the reaction was performed at 25 and 50 °C, the reaction yields were moderate. It was realized that the yield of benzo[4,5]imidazo[1,2-*a*] pyrimidin-2-one without catalyst is trace even at mixture of water/ethanol solvent. When different amounts of the catalyst were loaded it was indicated the optimum amount is 0.04 g. Finally, the optimum time for the reaction was 7 h in the presence of catalyst at 70 °C.

In order to extend the above reaction to a library of benzo [4,5]imidazo[1,2-*a*]pyrimidin-2-ones, various kinds of aryl aldehydes and anilines were subjected under optimum conditions (Scheme 4). The final products differed only according to the groups substituted in ortho, meta and para of the aldehyde and aniline. The reaction was performed both either electron-withdrawing and electron-donating groups. However, the reaction was not performed with aliphatic aldehydes and heterocyclic aldehydes such as *n*-butanal, *n*-heptanal, furfural, thiophene-2-carboxaldehyde and pyridine-4-carboxaldehyde under the optimized condition. Also, 2-aminobenzothiazole, 2-aminopyridine, 2-aminopyrimidine was used instead of 2-aminobenzimidazole, unfortunately the reaction did not proceed. Moreover, diethyl acetylenedicarboxylates (DEAD) and methyl propiolate was used instead of DMAD. DEAD acted exactly like DMAD and produced benzo[4,5]imidazo[1,2-*a*]

Scheme 3. A four-component reactions.

ChemistryOpen

Full Papers
doi.org/10.1002/open.202100063

Chemistry Europe
European Chemical
Societies Publishing

Table 2. Optimization of one-pot consecutive synthesis of the benzo[4,5]imidazo[1,2-a]pyrimidin-2-one.[a]

Entry	Solvent	Temperature/°C	Catalyst amount/g	Yields/%
1	Ethanol	reflux	–	0
2	Ethanol	70	0.04	42 (23)[b]
3	Methanol	reflux	0.04	45
4	Isopropanol	70	0.04	41
5	Acetonitrile	70	0.04	29
6	Solvent free	70	0.04	trace
7	H_2O	70	0.04	56
8	H_2O/EtOH	70	0.04	86 (86%)[c]
9	H_2O/EtOH	95	0.04	86
10	H_2O/EtOH	50	0.04	54
11	H_2O/EtOH	25	0.04	42
12	H_2O/EtOH	70	0.03	55
13	H_2O/EtOH	70	0.02	44
14	H_2O/EtOH	70	0.01	32
15	H_2O/EtOH	70	–	trace

[a] Aniline (0.5 mmol), DMAD (0.5 mmol), benzaldehyde (0.5 mmol), 2-aminobenzimidazole (0.5 mmol), NM-SiO$_2$@SiPA-MA-Arg@HPA, 20 h, solvent. [b] One-pot domino synthesis. [c] 7 h.

pyrimidin-2-ones (Scheme 4). While by methyl propiolate molecule, dimethyl 1-(1H-benzo[d]imidazol-2-yl)-4-phenyl-2,6-bis(phenylamino)-1,4-dihydropyridine-3,5-dicarboxylate was obtained (Scheme 5).

The structure of products **5 a–n** is deduced from their IR, ^{1}H NMR and ^{13}C NMR spectra and by elemental analysis. For example, the FT-IR spectrum of the **5 g** indicated the formation of benzoimidazo[1,2-a]pyrimidin-2-ones. The absorption bands around 3311 and 3112 cm^{-1} are related to amid N—H and amine N—H bonds, respectively. The vibrations bands at 2948 and 2874 cm^{-1} were assigned to the CH$_3$ part. The broad strong vibration signal at 1680 cm^{-1} is attributed to the stretching vibrations of carbonyl groups and bending vibrations of N—H groups. Stretching of the imine and vinyl bonds are at 1626 and 1496 cm^{-1} respectively. C—N, C$_{(SP^2)}$—O and C$_{(SP^3)}$—O bonds vibrate separately at 1389, 1228 and 1198 cm^{-1}. The ^{1}H NMR of the **5 g** product shows two singlets at 2.17 and 3.51 ppm for hydrogens of benzylic CH$_3$ group and methoxy (OCH$_3$) group, respectively. Another singlet is also appeared at 5.91 ppm that is related to hydrogen of C—H group. This CH locates among nitrogen and two aromatic rings. Aromatic hydrogens are seen at $\delta = 6.98$–7.28 as multiplet. Finally, two hydrogens amine and amid are observed as two close singlets at 7.56 and 7.58 ppm, respectively. On the other hand, ^{13}C NMR shows the production of final compound. ^{1}H-decoupled ^{13}C NMR spectrum of **5 b** shows the carbons of methyl, methine and methoxy are appeared at 20.06, 49.73 and 59.52 ppm, respectively. Aromatic carbons are observed at 110–136 ppm. Carbonyls of amide and ester functional groups resonate at 162.81 and 165.58 ppm, respectively. In any case, the number of carbon signals is less than the number of carbons which was expected due to the overlap of some carbons. Thus, elemental analysis was prepared from the sample and the results completely confirmed that the experimental value is very similar to theoretical value.
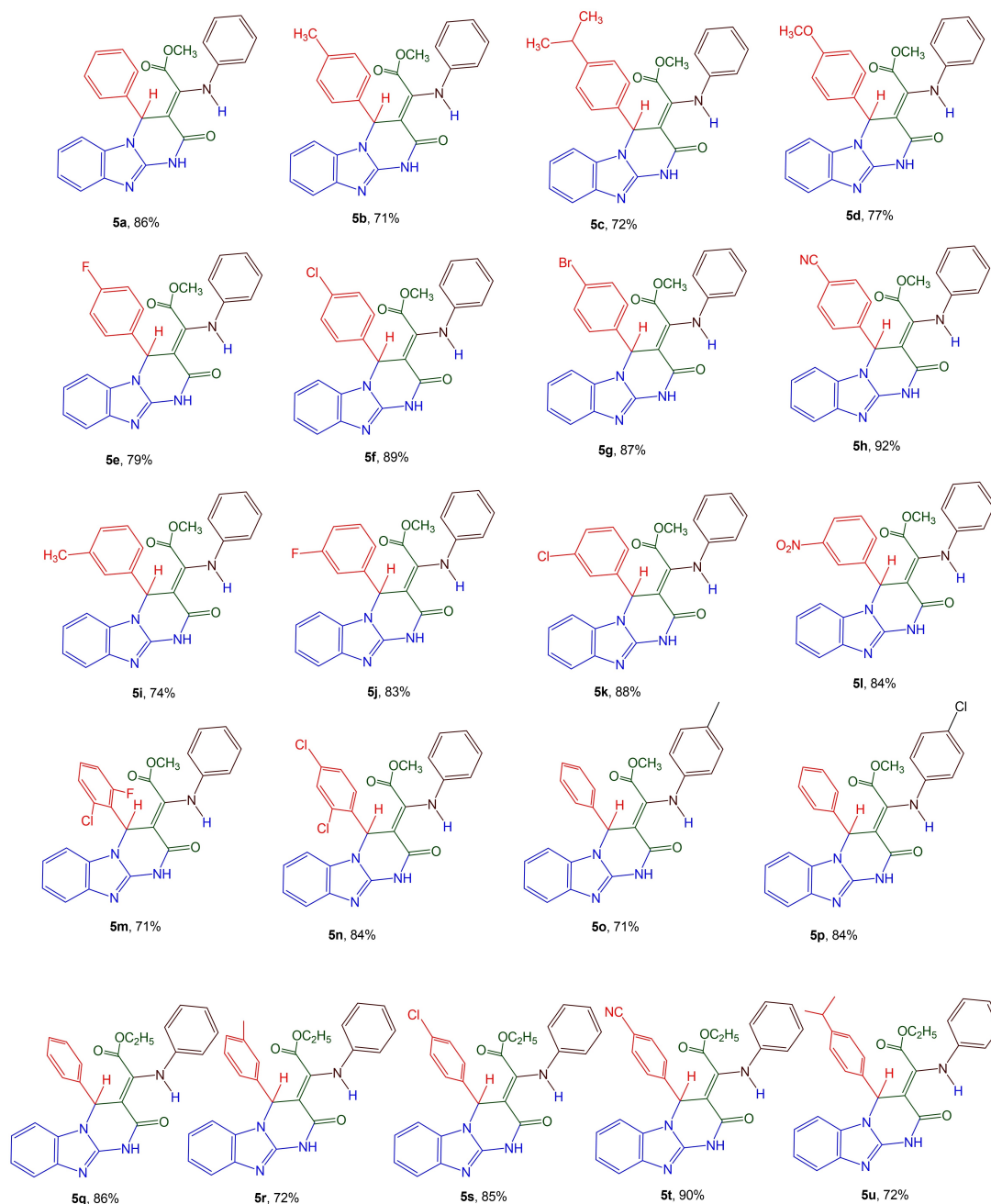
The possible mechanism for the synthesis of benzo[4,5]imidazo[1,2-a]pyrimidin-2-one has been shown in Scheme 6. At first, aniline (**1 a**) reacts quickly with DMAD (**2**) and gives enamine **8**. Then, enamine is condensed with an aldehyde which has been activated by the catalyst. In result, an α,β-unsaturated compound **9** is created by elimination of one water molecule. This α,β-unsaturated compound is activated again by the catalyst via linking onto the oxygen atoms. Next, the reaction is followed by Michael addition of 2-aminobenzimidazole to this active compound **10**, followed by compound **11** is synthesized and activated by catalyst once again. By intramolecular cyclization of compound **11**, the compound **12** is created. Finally, the final product (**5**) is obtained by elimination of a methanol molecule and other molecules and/or parts by removing the catalyst using a magnet.[42]
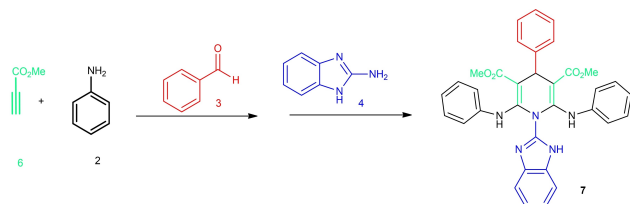
The reusability of NM-SiO$_2$@SiPA-MA-Arg@HPA catalyst was investigated up to six times in model reaction under optimized conditions. After each reaction, the catalyst is separated from the reaction medium by a magnet and washed with 20 ml of ethanol, to remove reactants and products adsorbed on the catalyst. After each time, it was dried in an oven at 100 °C for 2 h and used again with new substrates under the same conditions. The results showed that the catalyst can be reused several times due to the negligible decrease in the yields of the reactions (86 to 84%) (Figure 7A). The FT-IR spectrum and SEM images of the catalyst were obtained after six rounds (Figure 7B and 7C). FT-IR spectrum displayed the same signals in both of the fresh and final catalysts. Just like that, the SEM images revealed that the morphology and particle size of the catalyst have the identical shape before and after using of six times. Thus, these results show that this inorganic-organic hybrid catalyst is stable.

3. Conclusion

In summary, we have synthesized a new hybrid nanomagnetic catalyst that with excellent catalytic potential in the synthesis of the new benzo[4,5]imidazo[1,2-a]pyrimidin-2-one molecules via one-pot consecutive four components reaction. The high yields of products were due to a synergistic effect between high catalytic performance and hydrophobic effect of water solvent.
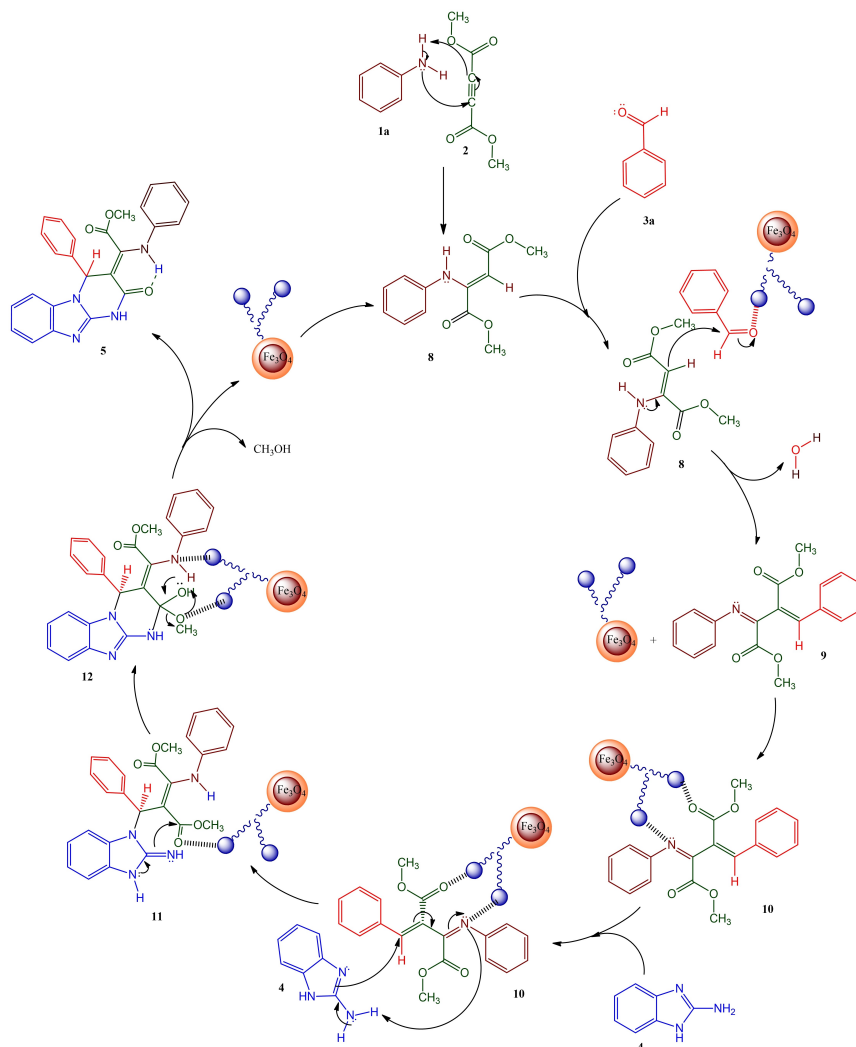
ChemistryOpen

Full Papers
doi.org/10.1002/open.202100063

Chemistry Europe
European Chemical
Societies Publishing

Scheme 4. Benzo[4,5]imidazo[1,2-*a*]pyrimidin-2-one derivatives using NM-SiO$_2$@SiPA-MA-Arg@HPA catalyst. Aniline (1 mmol), DMAD (1 mmol), benzaldehyde derivatives (1 mmol), 2-aminobenzimidazole (1 mmol), water/ethanol (5/1 mL), 70 °C.

Scheme 5. Synthesis of 1,4-dihydropyridine using methyl propiolate molecule in the presence of NM-SiO$_2$@SiPA-MA-Arg@HPA catalyst.

The presence of a long organic part caused the excellent dispersion of the catalyst in water solvent and easy flexibility of the catalyst. Using magnetic nanocatalyst facilitated the isolation and reusability. The use of water as a green solvent, a stable heterogeneous catalyst and excellent yields of the products as well as recyclability of the catalyst were the significant results of this work. Alternatively, production of new organic compounds with valuable heterocyclic parts including pyrimidine and imidazole rings is one of the main goals of sustainable organic chemistry. Therefore, we believe that this

ChemistryOpen

Full Papers
doi.org/10.1002/open.202100063

Chemistry Europe
European Chemical
Societies Publishing

Scheme 6. Suggested mechanism for the formation of benzo[4,5]imidazo[1,2-*a*]pyrimidin-2-one.

work opens a new path to green chemistry and organic synthesis.

Experimental Section

Synthesis of NM-SiO₂@SiPA-MA-Arg@HPA as Organic-Inorganic Hybrid Nano-Catalyst

Preparation of Fe₃O₄ magnetic nanoparticles (NMs)

Fe₃O₄ nanoparticles (NMs) were prepared according to the reported procedure in the literature.[54] The mixture of iron (III) chloride hexahydrate (4.6 g, 0.017 mol) and iron (II) chloride (2.2 g, 0.011 mol) was subjected in 100 ml of deionized water until the salts were completely dissolved. Then, 10 ml of aqueous ammonia was rapidly mixed in nitrogen atmosphere at 25 °C for about 30 minutes with a mechanical stirrer. The obtained precipitates were removed using a magnet and washed with distilled water several times.

Preparation of Nanomagnetic Particles Coated by Silica (NM-SiO₂)

This silica coated NMs have been synthesized using the Stöber method with some modifications.[55] The NM (1 g) was dispersed by the ultrasonic waves in 50 mL of distilled water at 20 min. Then, this suspension was added into 140 mL of ethanol, stirring at 40 °C. Next, 5 mL of NH₃.H₂O was poured into the obtained mixture. After that, 1 mL of TEOS was diluted in ethanol (20 mL) and added drop wise to this suspension. The resulting suspension was kept stirred mechanically for 14 h at room temperature. Then, this dispersed mixture was centrifuged at 6000 rpm for 30 min. The magnetic Fe₃O₄/SiO₂ nanoparticles were collected by a magnet and washed with ethanol and deionized water several times.

Preparation of Nanomagnet-SiO₂@silyl Propylamine (NM-SiO₂@SiPA)

As described in the literature,[56] NM-SiO₂@Si-PA was synthesized as follows: NM-SiO₂ (1.50 g) was further diluted with ethanol (200 mL) containing γ-amino propyl-triethoxysilane (13 mmol, 3 mL) under ultra-sonication in a water bath. The resultant dispersion was bubbled with argon gas for 30 min, and then heated at 40 °C under
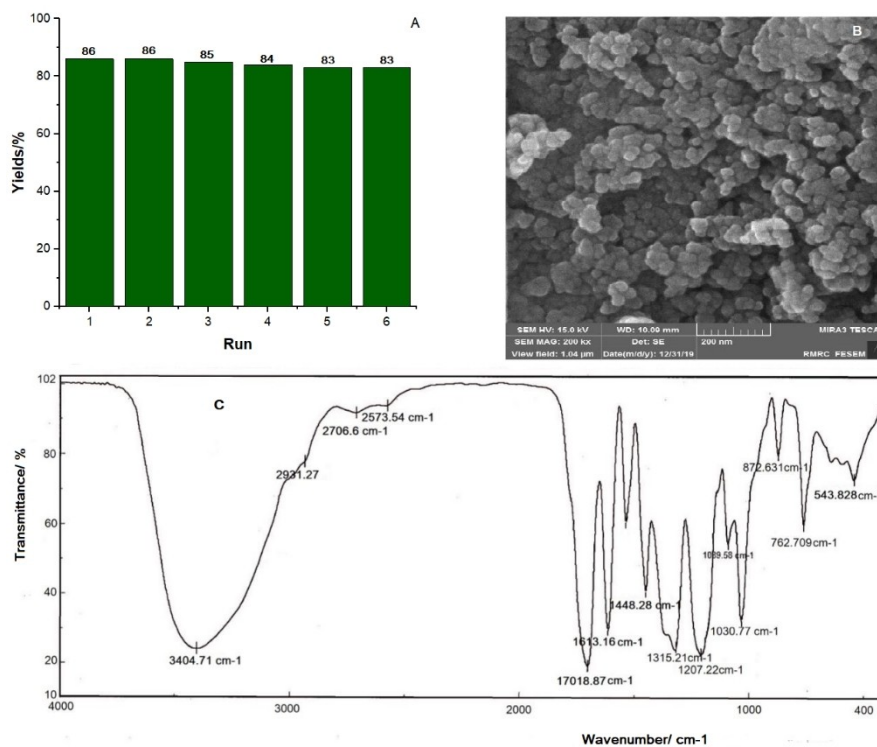
ChemistryOpen

Full Papers
doi.org/10.1002/open.202100063

Chemistry Europe
European Chemical
Societies Publishing

Figure 7. Recyclability of the catalyst (A), The SEM images (B) and FT-IR spectrum (C) after six rounds.

mild mechanical stirring for 24 h. Finally, the APTES-modified Fe_3O_4 nanoparticles were collected using a magnet and washed repeatedly with ethanol and deionized water. The precipitated products of NM-SiO_2@SiPA were dried at 30 °C under vacuum.

Preparation of Maleic Acid Functionalized Nanomagnet-SiO_2@silyl Propylamine (NM-SiO_2@SiPA-MA)

NM-SiO_2@SiPA (0.2 g) and excess amount of maleic anhydride were added to a test tube which was closed thermally and then placed in an oven at 100 °C for 24 h. The obtained product was washed three times with ethyl acetate and then dried.

Preparation of silica coated Fe_3O_4 nanomagnets@silyl propylamine-maleic acid-arginine salt (NM-SiO_2@SiPA-MA-Arg)

First, 1 mmol of arginine was treated with soda in a solution of methanol: with a ratio of 2:1. The obtained mixture was poured into a test tube containing 0.1 g of NM-SiO_2@SiPA-MA and then hermetically closed. After 5 hours at 120 °C, the obtained product was washed with distilled water and dried. The dry product was treated with excess hydrochloric acid converting the amine functions to ammonium salt, which facilitates complexion with negatively charged heteropolyacid.

Synthesis of Heteropolyacid (HPA)

A mixture of 8.33 mmol of sodium tungstate and 0.76 mmol of sodium hydrogen phosphate in 20 mL of distilled water was stirred until completely dissolved, and then the addition of 1 mmol of zinc nitrate. these three reagents were maintained under vigorous stirring for one hour at room temperature, then concentrated nitric acid was added until an acidic solution was obtained (pH = 4.8). Thus, a solution of heteropolyacid salt was obtained 51.

Final Synthesis of NM-SiO_2@SiPA-MA-Arg@HPA Catalyst

The last step of the synthesis of NM-SiO_2@SiPA-MA-Arg@HPA was adding the NM-SiO_2@SiPA-MA-Arg salt to the beaker containing the solution of the heteropolyacid salt. The rapid complexion of these two synthetic products made it possible to have the magnetic hybrid catalyst which was isolated using a magnet. Then, the synthesized catalyst was washed several times with distilled water.

General Procedure for the Preparation of Benzo[4,5]imidazo [1,2-*a*]pyrimidin-2-one Derivatives

DMAD or DEAD (1 mmol) was added to a 25 mL round-bottomed balloon containing aniline derivative (1 mmol) and water (5 mL) and stirred for 40 min at room temperature. Then, aromatic aldehyde (1 mmol) and the NM-SiO_2@SiPA-MA-Arg@HPA catalyst (0.04 g) were added to this mixture and stirred until a precipitate was appeared. Next, 2-aminobenzimidazole (1 mmol) poured out into this mixture. Subsequently, 1 mL of ethanol was added until dissolve the formed precipitate and 2-aminobenzimidazole. Progress of the reaction was monitored by TLC for 4 h. After completion of the reaction, mixture of the product and catalyst were filtered, washed and heated in ethanol. Then, the catalyst was removed by an external magnet. The pure crystals were obtained by the cooling of the solution.

Acknowledgements

Conflict of Interest

The authors declare no conflict of interest.

[1] P. Anastas, N. Eghbali, *Chem. Soc. Rev.* **2010**, *39*, 301.
[2] H. C. Erythropel, J. B. Zimmerman, T. M. de Winter, L. Petitjean, F. Melnikov, C. H. Lam, P. T. Anastas, *Green Chem.* **2018**, *20*, 1929.
[3] F. M. Kerton, R. Marriott, *Alternative Solvents for Green Chemistry*: Edition 2, *RSC*, **2013**.
[4] G. Yanlong, *Green Chem.* **2012**, *14*, 2091.
[5] R. A. Sheldon, *Green Chem.* **2005**, *7*, 267.
[6] F. Chemat, M. Abert Vian, H. K. Ravi, B. Khadhraoui, S. Hilali, S. Perino, A. S. F. Tixier, *Molecules.* **2019**, *24*, 3007.
[7] P. T. Anastas, C.-J. Li, *Green Solvents: Reactions in Water*, Volume 5, Wiley-VCH, **2013**.
[8] U. S. Ozkan, Design of heterogeneous catalysts: new approaches based on synthesis, charactrizations and modeling, Wiely-VCH, Weinheim, **2009**.
[9] R. A. van Santen, Modern Heterogeneous Catalysis: An Introduction, Wiely-VCH, **2017**.
[10] K. Wilson, A. F. Lee, Heterogeneous Catalysis for clean technology: Spectroscopy, Design, and Monitoring, Wiely-VCH, **2013**.
[11] S. Robert, *Angew. Chem. Int. Ed.* **2015**, *54*, 3465.
[12] I. V. Kozhevnikov, *Chem. Rev.* **1998**, *98*, 171.
[13] Y. Gu, *Green Chem. Lett. Rev.* **2012**, *14*, 2091.
[14] M. Almohalla, I. Rodríguez-Ramos, A. Guerrero-Ruiz, *Catal. Sci. Technol.* **2017**, *7*, 1892.
[15] R. Tayebee, M. M. Amini, H. Rostamian, A. Aliakbari, *Dalton Trans.* **2014**, *43*, 1550.
[16] J. Zhu, Q. Wang, M.-X. Wang, *Multicomponent Reactions in Organic Synthesis*, Wiley-VCH, **2015**.
[17] R. P. Herrera, E. Marqués-López, Multicomponent Reactions: Concepts and Applications for Design and Synthesis, Wiley-VCH, Hoboken New Jersey, **2015**.
[18] L. Banfi, A. Basso, R. Riva, R. V. A. Orru, E. Ruijter, *Synthesis of Heterocycles via Multicomponent Reactions I*, Springer-Verlag Berlin Heidelberg, **2010**.
[19] S. Zhi, X. Ma, W. Zhang, *Org. Biomol. Chem.* **2019**, *17*, 7632.
[20] A. F. S. Barreto, C. K. Z. Andrade, *Beilstein J. Org. Chem.* **2019**, *15*, 906.
[21] K. L. Ameta, A. Dandia, Multicomponent Reactions: Synthesis of Bioactive Heterocycles, CRC Press, **2017**.
[22] R. C. Cioc, E. Ruijter, R. V. A. Orru, *Green Chem.* **2014**, *16*, 2958.
[23] D. Y. Kim, P. D. Q. Dao, C. S. Cho, *ACS Omega.* **2018**, *3*, 17456.
[24] S. Sirko, N. Y. Gorobets, V. Musatov, S. Desenko, *Molecules* **2009**, *14*, 5223.
[25] V. V. Fedotov, E. N. Ulomskiy, E. B. Gorbunov, O. S. Eltsov, E. K. Voinkov, K. V. Savateev, R. A. Drokin, S. K. Kotovskaya, V. L. Rusinov, *Chem. Heterocycl. Compd.* **2017**, *53*, 582.
[26] O. Algul, A. Meric, S. Polat, N. Didem Yuksek, M. Serin, *Cent. Eur. J. Chem.* **2009**, *7*, 337.
[27] T. Chiba, S. Shigeta, Y. Numazaki, *Biol. Pharm. Bull.* **1995**, *18*, 1081–1083.
[28] H. Wahe, P. F. Asobo, R. A. Cherkasov, Z. T. Fomum, D. Doepp, *Arkivoc* **2004**, *8*, 130.
[29] K. Terashima, O. Muraoka, M. Ono, *Chem. Pharm. Bull.* **1995**, *43*, 1985.
[30] S. M. Sondhi, R. P. Verma, V. K. Sharma, N. Singhal, J. L. Kraus, M. Camplo, J.-C. Chermann, *Phosphorus Sulfur Silicon Relat. Elem.* **1997**, *122*, 215.
[31] R. Jorda, Eva Reznícková, U. Kiełczewska, J. Maj, J. W. Morzycki, L. Siergiejczyk, V. Bazgier, K. Berka, L. Rarov, A. Wojtkielewicz, *Eur. J. Med. Chem.* **2019**, *179*, 483.
[32] H. T. Abdel-Mohsen, F. A. F. Ragab, M. M. Ramla, H. I. El Diwani, *Eur. J. Med. Chem.* **2010**, *45*, 2336.
[33] A. Nowicka, H. Liszkiewicz, W. P. Nawrocka, J. Wietrzyk, K. Kempińska, A. Dryś, *Cent. Eur. J. Chem.* **2014**, *12*, 1047.
[34] S. M. Sondhi, S. Rajvanshi, M. Johar, N. Bharti, A. Azam, A. K. Singh, *Eur. J. Med. Chem.* **2002**, *37*, 835.
[35] S. Lazareno, *Mol. Pharmacol.* **2002**, *62*, 1492.
[36] U. B. Gangadharmath, H. C. Kolb, P. J. H. Scott, J. C. Walsh, W. Zhang, A. K. Szardenings, A. Sinha, G. Chen, E. Wang, V. P. Mocharla, C. Yu, C. Liu, D. Cashion, D. Kasi, *US Patent* 2013/0302248 A1.
[37] R. Kumar, P. F. Pavlov, B. Winblad, *J. Alzheimer's Dis.* **2020**, *73*, 695.
[38] C. Davidson, T. H. Lee, E. H. Ellinwood, *Eur. J. Pharmacol.* **2004**, *499*, 355.
[39] A. Da Settimo, G. Primofiore, F. Da Settimo, A. M. Marini, S. S. Taliani, Salerno, L. D. Via, *J. Heterocycl. Chem.* **2003**, *40*, 1091.
[40] M. W. Martin, J. Newcomb, J. J. Nunes, C. Boucher, L. Chai, L. F. Epstein, T. Faust, S. Flores, P. Gallant, A. Gore, Y. Gu, F. Hsieh, X. Huang, J. L. Kim, S. Middleton, K. Morgenstern, A. Oliveira-dos-Santos, V. F. Patel, D. Powers, P. Rose, Y. Tudor, M. M. Turci, A. A. Welcher, D. Zack, H. Zhao, L. Zhu, X. Zhu, C. Ghiron, M. Ermann, D. Johnston, C. G. P. Saluste, *J. Med. Chem.* **2008**, *51*, 1637.
[41] A. A. Abdel-hafez, *Arch. Pharmacal Res.* **2007**, *30*, 678.
[42] A. Shaabani, A. Rahmati, S. Naderi, *Bioorg. Med. Chem. Lett.* **2005**, *15*, 5553.
[43] J. Liu, M. Lei, L. Hu, *Green Chem.* **2012**, *14*, 840.
[44] J. Azuaje, J. Brea, O. Caamano, X. Garcia-Mera, H. Gutierrez-De-Teran, W. Jespres, M. I. Loza, E. Sotelo, C. Velando, *J. Med. Chem.* **2020**, *63*, 7721.
[45] B. Jismy, M. Akssira, D. Knez, G. Guillaumet, S. Gobec, M. Abarbri, *New J. Chem.* **2019**, *43*, 9961.
[46] P. H. Tran, T.-P. Thi Bui, X.-Q. Bach Lam, X.-T. Thi Nguyen, *RSC Adv.* **2018**, *8*, 36392.
[47] S. J. Kalita, D. Chandra Deka, H. Mecadon, *RSC Adv.* **2016**, *6*, 91320.
[48] X. Shang, M. Geng, L. Wu, *Asian J. Chem.* **2012**, *24*, 515.
[49] O. Rosati, M. Curini, F. Montanari, M. Nocchetti, S. Genovese, *Catal. Lett.* **2011**, *141*, 850.
[50] C. Yao, S. Lei, C. Wang, T. Li, C. Yu, X. Wang, S. Tu, *J. Heterocycl. Chem.* **2010**, *47*, 26.
[51] Z. Nadealian, V. Mirkhani, B. Yadollahi, M. Moghadam, S. Tangestaninejad, I. Mohammadpoor-Baltork, *J. Coord. Chem.* **2012**, *65*, 1071.
[52] R. Sadasivan, A. Patel, *RSC Adv.* **2019**, *9*, 27755.
[53] Y. Wu, X. Li, Y. Liu, G. Xiao, Y. Huang, Y. Li, D. Dang, Y. Bai, *RSC Adv.* **2019**, *9*, 11932.
[54] W. Stober, A. Fink, E. Bohn, *J. Colloid Interface Sci.* **1968**, *26*, 62.
[55] T. Zeng, L. Yang, R. Hudson, G. Song, A. R. Moores, C.-J. Li, *Org. Lett.* **2010**, *13*, 442.
[56] J. Wang, S. Zheng, Y. Shao, J. Liu, Z. Xu, D. Zhu, *J. Colloid Interface Sci.* **2010**, *349*, 293.